QUARTERLY JOURNAL OF THE ROYAL METEOROLOGICAL SOCIETY

Q. J. R. Meteorol. Soc. **00**: 1–25 (2007)

Published online in Wiley InterScience

(www.interscience.wiley.com) DOI: 10.1002/qj.000

Large scale potential vorticity anomalies and deep convection

A. Russell[a]*, G. Vaughan[b] and E. G. Norton[b]

[a]*Institute for the Environment, Brunel University, UK.* [b]*Centre for Atmospheric Science, University of Manchester, UK.*

Abstract:

The effect on deep convection of large scale potential vorticity (PV) anomalies and their associated tropospheric stable layers is complex and not well understood. This paper examines the meteorological events of 9 July 2007 (IOP 7b of the Convective and Orographically-induced Precipitation Study, or COPS), which was dominated by an upper-level PV anomaly that stretched from the UK to southern France and as far north-east as Denmark. Three precipitation regions were identified from the case: lines of intense storms beneath the PV anomaly; less intense, more widespread convective precipitation to the east of the PV anomaly; and, in between, a region of no precipitation. The latter of these coincided with the high resolution measurements and model analyses from COPS. The extensive and varied data analysed in this investigation show that convective available potential energy (CAPE) was present in this region (the distribution of CAPE and convective inhibition (CIN) is presented via an innovative, pseudo-3D visualisation that allows horizontal and vertical interactions to be considered). However, convection was capped by a complex arrangement of dry layers - the base of the key layer was at 750 hPa. These dry layers descended separately from the upper-troposphere, moving around the PV anomaly as it developed from a breaking Rossby wave to the west, during the 7 days before the IOP. This case adds to other studies that show that descent of complex dry layers is an important mechanism for forming convection-inhibiting atmospheric lids in Western Europe. A simple conceptual model is developed that synthesises the effect of large scale PV anomalies on deep convection from a series of consistent case studies. This model has significant implications for storm forecasting and projections of storminess in future climates as it highlights the importance of thin structures that can advect 100s km before having an impact.

KEY WORDS atmospheric lid; tropopause fold; convective inhibition; COPS

Received ; Revised ; Accepted

1 Introduction

Intense or prolonged precipitation can cause flooding and lead to disruption, damage to property and endanger lives. Therefore, improving quantitative precipitation forecasts is a key goal for meteorology. An important step in achieving this aim is to improve our understanding of the atmospheric processes leading up to such precipitation events. One important process in the development of convective storms involves upper-level potential vorticity (PV) anomalies and the tropospheric stable layers that originate from these anomalies.

This paper aims to build on the current understanding of the role of these features by describing a case where the upper-level features strongly influenced the convective

*Correspondence to: Andrew Russell, Institute for the Environment, Brunel University, Uxbridge, UB8 3PH, UK. E-mail: andrew.russell@brunel.ac.uk

environment. The goal in this particular case study is to understand the modulation of convection by the PV anomaly overhead and the dry layers in the troposphere that originated from that anomaly.

1.1 Convection and PV anomalies

Hoskins *et al.* (1985) reviewed the mechanisms by which upper-level potential vorticity (PV) anomalies can reduce the convective stability of the troposphere. Of greatest relevance is how the upward curvature of isentropes in the troposphere connected with a moving PV anomaly is associated with tropospheric ascent of air ahead of, and descent of air behind, the depressed tropopause. This ascent can contribute to the development of deep convection by release of potential instability (e.g. Browning and Roberts, 1994).

Further, the upward displacement of isentropic surfaces leads to an upper-level cold pool, which causes a reduction in static stability beneath the PV anomaly. This, under suitable conditions, will promote deep convection (e.g. Morcrette *et al.*, 2007).

1.2 Atmospheric lids

The role of atmospheric lids (or inversions, amongst other names) in the initiation of convection is not straightforward. The name implies that lids predominantly limit the development of convection but this is not always the case. For example, Graziano and Carlson (1987) conducted an analysis of lid strength versus severe storm activity over a six month period in 1982 for the central two-thirds of the USA. They showed that, when considering cases with a given value of buoyancy, the probability of deep convection increased with increasing lid strength. This implies that the presence of the lid allows convective available potential energy (CAPE) to build up beneath the lid to the point where intense, deep convection can occur.

Looking at specific cases, Russell *et al.* (2008 and 2009) have examined the role and origin of atmospheric lids in the UK from an observational field campaign — the Convective Storm Initiation Project, or CSIP, (Browning *et al.*, 2007). These studies showed that lids are important in the development and timing of convective storms and that they are difficult to model correctly or consistently. One case, CSIP IOP1 (Morcrette *et al.*, 2007; Russell *et al.*, 2008), saw an isolated storm develop beneath a small PV anomaly and a widespread lid. This case was successfully modelled by the 1.5 km resolution Met Office Unified Model (UM) because many of the key features, including the lid and a topographically forced surface convergence line, were well observed and incorporated into the model (Lean *et al.*, 2009). A second case, CSIP IOP9 (Russell *et al.*, 2009) involving a band of showers over Southern England, was comparatively poorly modelled by the same version of the UM. These showers were organised mostly by two descending dry layers, which the UM represented as too cool, in the wrong place and orientated incorrectly when compared with the observations (Russell *et al.*, 2009). The other key finding from these studies was that the lids originated a long way from the location of the storms. In both cases, the layers that formed the lids advected in over a period of days beginning from a breaking Rossby wave thousands of kilometres to the west of the UK. The dry layers then moved eastwards over the UK behind a cold front and ahead of and partially beneath an upper-level PV anomaly.

Whilst these CSIP cases investigated the links between the upper-level PV anomaly and the capping layers beneath them in some depth, there are other examples in the literature of such layers in the vicinity of PV anomalies and convection, such as Browning and Hill (1985), Griffiths *et al.* (1998), Browning and Roberts (1999), Reid

DOI: 10.1002/qj

and Vaughan (2004) and Bennett *et al.* (2008). No similar cases have been reported for continental Europe.

A deeper understanding of all features involved in such cases, including this COPS case, is important for the development of numerical weather prediction (NWP) models — particularly as the lids can develop well outside of most models' mesoscale domain. See Browning *et al.* (2007) and Wulfmeyer *et al.* (2008) for further discussion about the development of NWP models using observations from CSIP and COPS.

1.3 Aims

The specific questions that this study addresses are:

(i) What was the structure and evolution of the upper-level (and upper-level derived) features affecting the convection in this case?

(ii) How did these upper-level features influence the convection and precipitation pattern observed?

(iii) How does this case improve our understanding of similar cases?

Point iii) is particularly important as severe precipitation events are often accompanied and promoted by upper-level PV anomalies (Roberts, 2000) and their associated tropospheric dry layers — i.e. the "dry intrusion" (Danielsen, 1964). The current case is useful with this aim in mind as there are three distinct precipitation regimes to examine, all forced by similar synoptic conditions.

2 The Convective and Orographically-induced Precipitation Study (COPS)

The case being investigated in this paper took place during COPS. This was an international scientific campaign that ran in and around the Black Forest region of Southern Germany (Fig. 1) for June, July and August in 2007. The main aim of COPS is to improve forecasts of convective precipitation, particularly in regions where orography plays a major role. COPS ran alongside a World Weather Research Program (WWRP) Forecast Demonstration Project (Demonstration of Probabilistic Hydrological and Atmospheric Simulation of flood Events in the Alpine region, or D-PHASE).

COPS has been summarised by Wulfmeyer *et al.* (2008) who also give a full breakdown of the instruments deployed at each of the supersites, which are identified in Fig. 1, and across the wider region.

3 Data

To analyse the vertical structure of the upper-level features and the convective stability of the region we use data from many radiosoundings and a UHF wind profiling radar (Norton *et al.*, 2006), which was located at Achern as part of Supersite R (8.07°E, 48.63°N). In the absence of precipitation, the UHF radar echo power depends on refractive index (RI) inhomogeneities, requiring either vertical gradients in potential temperature and specific humidity or active turbulence mixing together air of differing RI. Atmospheric lids meet the first of these conditions and are therefore manifest as layers of enhanced echo power.

The larger scale context is investigated using: European Centre for Medium Range Weather Forecasting (ECMWF) operational analyses; back trajectories driven by the ECMWF data; the Total Ozone Mapping Spectrometer, or TOMS (Heath *et al.*, 1975); and the Meteosat Second Generation (MSG) satellite, specifically Meteosat-8 (Schmetz *et al.*, 2002). TOMS detects undulations of the troposphere as maxima or minima in total ozone, presenting a complementary view to the Meteosat water vapour images and ECMWF data.

DOI: 10.1002/qj

4 COPS IOP 7b

4.1 Precipitation pattern

Figure 2(a) shows the three precipitation regimes present over and around the COPS area at 1200 UTC on 9 July 2007 (i.e. COPS IOP 7b). Over most of France, southeast Britain, northwest Germany and the Benelux nations there were lines of small but intense storms. Eastern Switzerland and southeast Germany experienced generally less intense but more widespread precipitation than the areas to the west. In between these two precipitation regimes, almost directly over the COPS area and extending north and south, there was a region free from precipitation.

Given the overall aims of the COPS project (see Section 2), we will begin this investigation with a qualitative assessment of how some of the D-PHASE models represented the precipitation pattern. Fig. 3 shows the precipitation field from five of the D-PHASE models. Comparison with the rainfall rate observed by radar (Fig. 3(f)) shows that none of the models recreates the observations well. Table I summarises the salient features of each model and briefly notes their shortcomings in representing the precipitation field (the reasons are discussed in Section 7). This comparison illustrates the difficulties that NWP models face in representing a precipitation pattern heavily influenced by an upper-level PV anomaly. Here we concentrate on one challenge for the models: the role of thin stable layers of stratospheric origin in the troposphere in inhibiting the development of convection.

4.2 Synoptic situation

How can this precipitation pattern be explained? Figure 4(a) shows a weak low pressure centre over eastern Europe and a region of high pressure pushing eastwards towards northern Spain: neither the intense showers over the UK and France nor the more widespread rainfall over South East Germany were associated with a well-developed surface cyclone. The location of the rainfall swathe to the east was, however, largely determined by the potential instability in this area related to a weak, quasi-stationary front.

Figure 4 also shows a large upper-level potential vorticity anomaly, located over the UK, France, the Benelux countries and extending as far north-east as Denmark. Figure 5 presents the MSG water vapour image for this time, together with the upper-level PV. Clearly, the PV anomaly was spatially correlated with convective activity.

Figure 5 also shows a dry filament, extending from northern Spain to the Alps and over the COPS region. The location of this dry filament correlates well with the region of no precipitation and, as we show later, was key to inhibiting convection in the COPS region. Firstly, though, the convective environment will be examined in more detail.

5 Convective stability of the troposphere

The three precipitation regimes discussed in the previous section can be summarised by three radiosoundings. Figure 6(a) represents the region where lines of convective storms were present. There was high CAPE in this sounding (400 J kg^{-1}) and zero convective inhibition (CIN). The high values of CAPE arise from the low temperatures in the upper-troposphere associated with the upper-level cold pool, as can be seen by comparing Figs. 6(a) and (b): despite the tropopause being at approximately the same height in the two profiles, the Trappes (Fig. 6(a)) profile was up to 8°C colder than the Achern profile (Fig. 6(b)) in the upper troposphere. Indeed, Fig. 7, which will be discussed in more detail later, shows the structure of the PV anomaly and the modulation of isentropes beneath it i.e.

DOI: 10.1002/qj

the sharp upper-tropospheric potential temperature gradient between Trappes and Achern.

Figure 6(b) shows the Achern sounding — this is a high resolution COPS sounding as opposed to the GTS data shown in (a) and (c), which only provide data on significant levels. There is evidence of multiple dry layers throughout the profile with very weak inversions at approximately 875 hPa and 800 hPa. Above these small inversions there was a much more pronounced lid, which was not breached during the day at this location despite the very low CIN (9 J kg^{-1}). This is consistent with the lack of precipitation in this area, although, if this lid had been penetrated, the resulting convection would have reached a further inversion at 450 hPa. The vertical extent of CIN for this main lid was between 700 and 630 hPa; its base was at around 750 hPa; and the dry layer extended up to 500 hPa. Within this dry layer, there is some significant sub-structure. In particular, the base layer (750–700 hPa) appears as though it could be a separate feature from the rest of the dry layer: there is a slight moistening of the layer at 700 hPa and there is a small inversion that peaks at about 725 hPa.

The presence of a lid in the upper-troposphere in the vicinity of a PV anomaly, as seen in the 1057 UTC Achern sounding at 450 hPa, has been observed previously by Reid and Vaughan (2004) and Russell *et al.* (2009) but in both those cases the convection reached the uppermost lid.

The third regime was characterised by the precipitation to the east of the COPS area. The final sounding, Fig. 6(c), shows a profile on the edge of the precipitation zone. It was nearly saturated at all levels above the boundary layer, which was itself more moist than seen in the other two soundings presented here. Nonetheless, there is still some CAPE to be released (210 J kg^{-1}) and there is almost no CIN (1 J kg^{-1}).

6 Role, structure and origin of the atmospheric lid

In this section we will show that the thick lid (i.e. the dry, stable layer seen in Fig. 6(b)) was key in determining the precipitation distribution over the western parts of Germany at 1200 UTC on 9 July 2007 where no precipitation was observed.

6.1 The dry layer over the COPS area

Whilst Fig. 6(b) demonstrated the structure and location of the the main dry layer at a single time in the COPS area, Fig. 8 uses data from the UHF radar and further radiosonde launches from Achern to examine the temporal development of convection at this site in relation to the main lid. Some of the other, less significant lids can also be investigated using this data.

The radar can measure the development of the convective boundary layer as well as dry layers at higher altitudes. Up to 0730 UTC there was a mixed layer below 500 m and two distinct layers of increased echo power. The lower of these ($<$1 km) was a residual layer, which was entrained into the mixed layer by 0800 UTC. This residual layer was not seen in soundings further to the south of Achern.

The upper layer tracks the base of the dry layer, as shown by the radiosondes (red-orange contours). This layer, which starts at around 3 km at 0400 UTC, corresponds to the base (i.e. where the humidity gradient is highest) of the largest inversion seen in Fig. 6(b). On two occasions, 0830 and 1130 UTC, convection reaches this level and is capped by the inversion. In the afternoon however, convection reaches well short of the dry air — it is now capped by an increase in the static stability at 800 hPa not associated with a layer of dry air. Furthermore, the

DOI: 10.1002/qj

air in the dry layer gradually becomes less dry and, being higher as well, is no longer visible in the radar echoes.

The changing height of the base of this dry layer above Achern over the period examined (i.e. high-low-high) is consistent with the Danielsen (1964) model of the dry intrusion (Fig. 9) and results from the position of the dry intrusion in relation to its associated cyclone during development (Browning and Roberts, 1999).

Although the radar gives a clear depiction of the dry layer until mid-day, the evidence that the layer capped convection in the COPS area and beyond is less obvious. To examine the wider area around the radar we present Fig. 10: a cloud-top height map derived from MSG at 1400 UTC. This clearly shows a hole in the cloud over Achern, but a narrow band of capped convection, indicated by the brown and dark green colours extending approximately south-southwest from Achern, which corresponds to the dark band on the water vapour image in Fig. 5. The brown colour denotes cloud tops between 10,000 ft (3 km) and 15,000 ft (4.5 km), consistent with the base of the dry layer at this time (3.3 km). This confirms that the main lid was indeed responsible for capping convection along the flank of the main PV anomaly. It is likely that the residual layer (875 hPa) at Achern, but not present further south, inhibited the early development of the convection there and explains why the convection did not reach the main lid at Achern in the afternoon. Nonetheless, the radar profile is a key illustration of the dry layer even if it does not show the capping.

6.2 Larger scale structure of the dry layers

Sections 5 and 6.1 have shown that the main lid capped convection in the COPS area but to understand its wider significance we need to look on larger scales. In order to assess the area affected by the lid we have analysed as much radiosonde data from the wider area as possible.

In Fig. 11 we present the distribution of CAPE and CIN in the lowest 500 hPa for each sounding available in the relevant areas giving a pseudo-three dimensional view of the convective environment. The plot can be viewed in light of the regimes discussed in previous sections of this paper; these regimes have been identified objectively on Fig. 11 using fields from the ECMWF data:

(i) soundings bounded by the red contour (2 PVU on the 315 K isentropic surface) and the western and northern extents of the plot correspond to the lines of intense convection and show high CAPE with little CIN;

(ii) soundings in line with the green contoured areas (50% RH on the 700 hPa surface) correspond to the region where convection was capped and show a layer of CIN;

(iii) soundings around the yellow contour (90% RH on the 900 hPa surface) correspond to the moist regions where widespread precipitation was observed and generally show high CAPE, though some show high CIN due to the cold surface conditions associated with the storm.

This novel presentation method gives a clear view from the COPS radiosonde data of the narrow, but nonetheless important, extent of the capping that was described in section 6.1.

6.3 Origin of the dry layer

With a view to understanding the vertical structure and potential origin of the lid in more depth, Fig. 12 shows a vertical cross section of RH around the edge of the PV anomaly and through the lid. Along the entire cross section it is clear that the boundary layer is particularly moist (>80%), which, given sufficient CAPE and low-level lifting, would pre-dispose the atmosphere to deep

DOI: 10.1002/qj

convection at any point — this is consistent with our interpretation of the data presented in Section 5. Indeed, in the 0–4°E portion of Fig. 12 (i.e. the region on the edge of the storms over France), a consistent moist column has developed well above the boundary layer as a result of the convection. However, for the 6–15°E portion there is a dry layer capping the low-level convection below 700–800 hPa. These aspects of the vertical structure were not clear from Fig. 5 as the MSG water vapour channel is most sensitive to the height range of 600–300 hPa, though it is quite clear from the MSG cloud top height data (Fig. 10).

This dry layer corresponds to the main lid identified in Figs. 6(b) and 8, the base of which was seen at around 750 hPa at Achern. It can also be seen as a high PV fragment in Fig. 7 at around 650 hPa, 15°E. The apparent descent observed in this case as the layer moved eastwards over the radar is, again, consistent with the Danielsen (1964) model of the dry intrusion (Fig. 9). Figure 12 also shows that the dry layer, in fact, appears to be two layers that are joined at around 7°E. This is consistent with the observations we made about the sub-structure of the dry layer in Section 5. In the rest of this paper we will refer to the two parts of this dry layer as the "main dry layer" (from 700 to 500 hPa) and the "base layer" (from 750 to 700 hPa), the latter of which was most important in capping the convection. This structure is similar to the complex arrangement of dry layers around another large scale PV anomaly observed during CSIP (Russell *et al.*, 2009).

As previously discussed, the synoptic situation in the region was dominated by the upper-level PV anomaly and we now examine the hypothesis that the key layers in this case also originated from upper levels. Figure 13 gives a PV perspective of the build up to COPS IOP7b. The main feature to note in Fig. 13 is the activity of the cut-off low (COL) over the Atlantic (approximately centred on 23°W, 52°N in Fig. 13(d)) — this COL developed from an LC2 type breaking Rossby wave (Thorncroft *et al.*, 1993) which developed outside of the time window shown here. The breaking Rossby wave produced a tropopause fold (Fig. 7 shows the complex legacy of this fold) and this resulted in the descent of dry, high-PV air from the upper-levels (Danielsen, 1964). This can be seen as the main dry layer in Fig. 6(b) and the mid-tropospheric dry layer over the COPS region in Fig. 12.

From examination of back trajectories (BTs) run from the height of the main dry layer and the base layer at 1200 UTC on 9 July 2007 (Fig. 14 and the circles plotted on Fig. 13), it can be seen that the base layer of the lid seen on Fig. 6(b) was derived from the same COL as the main dry layer. However, it only joined the same track as the main dry layer at around 35°W, 47.5°N and descended from around 500 hPa. A similar track can also be seen on MSG water vapour images, such as that shown in Fig. 5 i.e. the dry track described previously that can be seen over Northern Spain. Series of these MSG images (not shown) indicate that this dry filament started at around 40°W, 65°N and then flowed southeastwards over the Atlantic until it curved around the southern flank of the COL over northern Spain and then northwards towards the COPS region, as also seen in the BTs. From here, the BTs show that it descended under the main dry layer (i.e. the tropopause fold associated with the COL, see Fig. 7) and, therefore, resulted in the arrangement of dry layers that has been described in this paper. We have also produced an animation that combines Figs. 13 and 14 to aid understanding of the origin of the lid. The animation has been provided as supplementary material with this paper.

DOI: 10.1002/qj

This analysis shows that the dry layers often found in between mid-latitude fronts and upper-level PV anomalies are complex in structure and derived from multiple sources. Indeed, a similar arrangement of dry layers derived from tropopause folds was also described by Russell *et al.* (2009) in a similar case. The subtle and important differences between these cases that add to our understanding of the morphology of such features will be discussed in section 7.

7 Discussion and conceptual model

The overall aim of this paper was to investigate the links between large scale PV anomalies and deep convection. This was done within the framework of COPS but we were building on significant findings from CSIP. The CSIP work implied that more needed to be understood about the full role of such upper-level forcing, including features derived from the upper-levels and what happens on the fringes of these anomalies — this case addresses these issues.

The COPS case investigated here involved a large PV anomaly over much of western Europe, although not directly over the COPS region. Investigation using the ECMWF operational analyses and radiosonde data showed that the impact on convection directly beneath the PV anomaly was in line with the model presented by Hoskins *et al.* (1985) — the upper-level cold pool destabilised the vertical profile to such an extent that there was high CAPE ready to be released. This finding is also consistent with most of of the literature concerning similar convective events, in particular, the investigation into CSIP IOP1 (Morcrette *et al.*, 2007; Russell *et al.*, 2008).

The COPS region lay between the heavy showers associated with the PV anomaly to the west and a swathe of more widespread precipitation to the east. This makes our investigation particularly important as there are very few cases in the literature that focus on the inhibition of convective storms. Indeed, the Carlson and Ludlam (1968) model, which describes the development of severe local storms in western Europe, shows the necessary capping inversion originating via differential advection involving a southerly airstream from lower levels over arid regions. This model is in contrast with our findings here, as well as those from Russell *et al.* (2008 and 2009). In this respect, we propose a complementary model of lid origin in Western European severe storms.

The model, summarised in Fig. 15, is based upon the findings in this COPS case and the two CSIP cases investigated in previous papers, which follow a quite similar large scale pattern. This starts with a breaking Rossby wave over the Atlantic that results in a COL. This COL has a tropopause fold associated with it and, as the COL travels towards western Europe over a number days, upper-level air flows down the fold and into the mid- to low-troposphere where it forms the dry intrusion behind a cold front that precedes the COL. The intrusion is presented here as a simple layer despite the significant substructure that we have investigated. However, these second order attributes are, from our current understanding, variable to the point that their features cannot be generalised in a meaningful way. Nonetheless, our model indicates where this complex layer is to be found — its particular structure and role in individual/groups of cases remains to be determined.

It could be argued that most western European convective storms that are driven in some part by a PV anomaly will be accompanied by a dry layer/layers of

DOI: 10.1002/qj

upper-level origin as that layer is a by-product of the process that resulted in the PV anomaly. As such, by studying cases associated with PV anomalies as we have done with CSIP and COPS, the accompanying dry layer will be of the upper-level type instead of a dry layer originating via differential advection, as suggested by Carlson and Ludlam (1968). Equally, though, there are currently no statistics on the origin of the capping inversion involved in Western European storms so, at this stage, we can do no more than highlight the gap in our knowledge and plan research for the future to fill that gap. However, Roberts (2000) has shown that approximately 60% of western European storms are related to PV anomalies and there are other cases in the literature of PV anomalies, lids and deep convection being co-located (see Section 1.2). Therefore, this is likely to be an important mechanism in Western Europe.

The PV and humidity structures seen in these cases are often very complex. For example, Figs. 6(b) and 7 show multiple layers (tropopause folds) extruded from the main PV anomaly (one of which gave rise to the lid under examination here). For this reason, Fig. 15(c) shows a small fragment between the COL and the Rossby wave remnant to signify the potential for this complex structure.

There are, however, also many differences between the PV anomalies and their impacts that we have investigated. The main difference is that the dry layer in this COPS case was largely responsible for inhibiting the convection whereas, in the CSIP IOP9 case (Russell *et al.*, 2009), the motion of the dry layer helped to initiate a band of storms via its influence on the potential instability. Looking to CSIP IOP1 (Russell *et al.*, 2008) the differences were even greater. In terms of size, the CSIP IOP1 upper-level PV anomaly was about 500 km in diameter, in CSIP IOP9 it was about 1000 km in diameter and in COPS IOP7b 1500 km (see Fig. 13). As for the role of the lid in CSIP IOP1, it would have capped convection completely beneath the PV anomaly were it not for the extra forcing of a convergence line and orographic effects on the cloud cover that led to the development of an isolated storm.

Despite these differences, there is enough common ground between these cases to present a conceptual model summarising the link between large scale PV anomalies and deep convection (Fig. 15). This model also includes the areas of uncertainty in this field — research is ongoing to reduce the uncertainty and to identify the climatological importance of the mechanism described.

Clearly, from just these three examples, there is a wide variety of PV anomaly type and dry layer effect, which one would expect to present a challenge for NWP models. In the CSIP cases, it was shown that the Met Office Unified Model (UM) performed very well in IOP1 (Morcrette *et al.*, 2007) but the UM representation was less good when compared with observations from the IOP9 case (Russell *et al.*, 2009). Whilst the D-PHASE models examined for COPS IOP7b case (Fig. 3) all captured various aspects of the precipitation well, they all had problems with certain characteristics (see Table I). Much of this difference may stem from parametrisation schemes (Figs. 3(a) and (b)) or domain edge effects (Figs. 3(d) and (e)). However, inspection of other fields from these model runs shows that all the models failed to represent the dry layers well. This was despite all capturing the main PV anomaly approximately correctly. This is the same issue identified by Russell *et al.* (2009) and is very likely to have affected the regions where convection was capped in the models and, therefore, where precipitation developed. This implies that this is an area of NWP

DOI: 10.1002/qj

model development that still requires work but that success should be possible as all the features we have investigated work on relatively large scales. This also applies to climate models, such as those being used in the 5th Coupled Model Intercomparison Project (CMIP5; http://cmip-pcmdi.llnl.gov/cmip5/), which are now reaching the level of vertical and temporal resolution required to capture these layers and allow an assessment of how they may modify the future severe storm environment.

8 Conclusions

In this paper we have investigated the precipitation patterns seen over and around the COPS area on 9 July 2007 (IOP 7b). This was split into three distinct regimes: lines of small but intense storms beneath the centre of a large PV anomaly that was over much of western Europe; less intense but more widespread precipitation to the east of the PV anomaly; and in between these two regimes, there was a region of no precipitation. The capping between the two regions of precipitation was caused by a complex arrangement of dry layers, two of which had descended concurrently from the upper-troposphere whilst the large PV anomaly developed in days leading up to the IOP.

Whilst the dry intrusion and differential advection of dry layers are well understood in general terms, our investigation shows a level of detail that is not usually presented or appreciated. As the resolution of NWP models improves, these fine scale characteristics will need to be captured to produce accurate forecasts. Continued investigation into the origin, structure and impact of these features is required.

Acknowledgements

We would like to thank all the COPS team for the smooth running of the campaign and the high quality data that was collected. Thanks are also due to the Natural Environment Research Council (NERC) for supporting UK-COPS and the Facility for Ground-based Atmospheric Measurements (FGAM). The UK Met Office provided the Nimrod data shown in Fig. 2. NASA provided the TOMS ozone data shown in Fig. 4(b) via their web interface: http://toms.gsfc.nasa.gov. The British Atmospheric Data Centre (BADC) provided the MSG image (Fig. 5), the ECMWF data (Figs. 4(a), 5, 7, 11, 12, 13 and 14) and the back trajectories (Fig. 14) via their web trajectory service. The University of Wyoming provided some of the radiosonde data used in Fig. 11. The model data presented in Fig. 3 was produced by: a) Eric Bazile (Meteo-France); b) Jean-Pierre Chaboureau and Evelyne Richard (University of Toulouse); c) Ronald McTaggart-Cowan (Environment Canada); d) Felix Ament and Marco Arpagaus (MeteoSwiss) and; e) Michael Baldauf (Deutscher Wetterdienst). Finally, the constructive and insightful comments of the anonymous reviewers significantly improved the focus and structure of the paper — we are particularly grateful for their efforts.

References

Bennett LJ, Blyth AM, Browning KA, Norton EG. 2008. Observations of the development of convection through a series of stable layers during the Convective Storm Initiation Project. *Q. J. R. Meteorol. Soc.* **134** : 2079-2091.

Browning KA, Blyth AM, Clark PA, Corsmeier U, Morcrette CJ, Agnew JL, Ballard SP, Bamber D, Barthlott C, Bennett LJ, Beswick KM, Bitter M, Bozier KE, Brooks BJ, Collier CG, Davies F, Deny B, Dixon MA, Feuerle T, Forbes RM, Gaffard C, Gray MD, Hankers R, Hewison TJ, Kalthoff N, Khodayar S, Kohler M, Kottmeier C, Kraut S, Kunz M, Ladd DN, Lean MW, Lenfant J, Li Z, Marsham J, Mcgregor J, Mobbs SD, Nicol J, Norton E, Parker DJ, Perry F, Ramatschi M, Ricketts HMA, Roberts NM, Russell A, Schulz H, Slack EC, Vaughan G, Waight J, Wareing DP, Watson RJ, Webb AR, Weiser A. 2007. The convective storm initiation project. *Bull. Am. Meteorol. Soc.* **88** : 1939-1955.

DOI: 10.1002/qj

Browning KA, Hill FF. 1985. Mesoscale analysis of a polar trough interacting with a polar front. *Q. J. R. Meteorol. Soc.* **111** : 445462.

Browning KA, Roberts NM. 1994. Use of satellite imagery to diagnose events leading to frontal thunderstorms: part I of a case study. *Meteorol. Appl.* **1** : 303-310.

Browning KA, Roberts NM. 1999. Mesoscale analysis of arc rainbands in a dry slot. *Q. J. R. Meteorol. Soc.* **125** : 34953511.

Carlson TN, Ludlam FH. 1968. Conditions for the occurrence of severe local storms. *Tellus* **20** : 203-226.

Danielsen EF. 1964. *Project Springfield Report*. Defence Atomic Support Agency, Washington D.C. 20301, DASA 1517 (NTIS # AD-607980), 97pp.

Graziano TM, Carlson TN. 1987. A statistical evaluation of lid strength on deep convection. *Weather Forecast.* **2** : 127-139.

Griffiths M, Reeder MJ, Low DJ, Vincent RA. 1998. Observations of a cut-off low over southern Australia. *Q. J. R. Meteorol. Soc.* **124** : 11091132.

Heath DF, Krueger AJ, Roeder HA, Henderson BD. 1975. The solar back-scatter ultraviolet and total ozone mapping spectrometer (SBUV/ TOMS) for Nimbus G. *Opt. Eng.* **14** : 323-331.

Hoskins BJ, McIntyre ME, Robertson AW. 1985. On the use and significance of isentropic potential vorticity maps. *Q. J. R. Meteorol. Soc.* **111** : 877-946.

Lean HW, Roberts NM, Clark PA, Morcrette CJ. 2009. The surprising role of orography in the initiation of an isolated thunderstorm in Southern England. *Mon. Weather Rev.* **137** : 3026-3046.

Morcrette CJ, Lean H, Browning KA, Nicol J, Roberts N, Clark PA, Russell A, Blyth AM. 2007. Combination of mesoscale and synoptic mechanisms for triggering of an isolated thunderstorm: a case study of CSIP IOP 1. *Mon. Weather Rev.* **135** : 3728-3749.

Norton EG, Vaughan G, Methven J, Coe H, Brooks B, Gallagher M, Longley I. 2006. Boundary layer structure and decoupling from synoptic scale flow during NAMBLEX. *Atmos. Chem. Phys.* **6** : 433-445.

Reid HJ, Vaughan G. 2004. Convective mixing in a tropopause fold. *Q. J. R. Meteorol. Soc.* **130** : 11951212.

Roberts NM. 2000. The relationship between water vapour imagery and thunderstorms. JCMM Internal Report, No. 110, 40 pp.

Russell A, Vaughan G, Norton EG, Ricketts HMA, Morcrette CJ, Hewison TJ, Browning KA, Blyth AM. 2009. Convection forced by a descending dry layer and low-level moist convergence. *Tellus* **61A** : 250-263.

Russell A, Vaughan G, Norton EG, Morcrette CJ, Browning KA, Blyth AM. 2008. Convective inhibition beneath an upper-level PV anomaly. *Q. J. R. Meteorol. Soc.* **134** : 371-383.

Schmetz J, Pili P, Tjemkes S, Just D, Kerkmann J, Rota S, Ratier A. 2002. An introduction to Meteosat Second Generation (MSG). *Bull. Am. Meteorol. Soc.* **83** : 977-992.

Thorncroft CD, Hoskins BJ, McIntyre ME. 1993. Two paradigms of baroclinic-wave life cycle behaviour. *Q. J. R. Meteorol. Soc.* **119** : 1755.

Wulfmeyer V, Behrendt A, Bauer H-S, Kottmeier C, Corsmeier U, Blyth A, Craig G, Schumann U, Hagen M, Crewell S, Di Girolamo P, Flamant C, Miller M, Montani A, Mobbs S, Richard E, Rotach MW, Arpagaus M, Russchenberg H, Schlussel P, Konig M, Gartner V, Steinacker R, Dorninger M, Turner DD, Weckwerth T, Hense A, Simmer C. 2008. The Convective and Orographically Induced Precipitation Study. *Bull. Am. Meteorol. Soc.* **89** : 1477-1486.

DOI: 10.1002/qj

Table I. Summary of five of the D-PHASE models run for COPS IOP 7b and a qualitative assessment of the models' representation of the precipitation regimes.

Fig. no.	Model name	Institution	Resolution	Convection permitting?	Initial conditions	Representation of precipitation regimes compared to observations
3a	ALADIN	Meteo-France	11 km	No	ARPEGE	Precip. swathe too far SW; convective precip. too widespread, including over COPS region.
3b	MESO-NH	University of Toulouse	8 km	No	ARPEGE	All precip. too widespread, including over COPS region.
3c	GEM-LAM	Environment Canada	2.5 km	Yes	GEM	Convection lines over France but also over COPS region; precip. swathe right shape.
3d	COSMO-CH	MeteoSwiss	2.2 km	Yes	COSMO-EU	Precip. swathe in right place; convective precip. too weak and too late; no precip. over COPS area though.
3e	COSMO-DE	Deutscher Wetterdienst	2.8 km	Yes	COSMO-EU	Convection lines over France but too weak; precip. swathe in right place; no precip. over COPS area.

DOI: 10.1002/qj

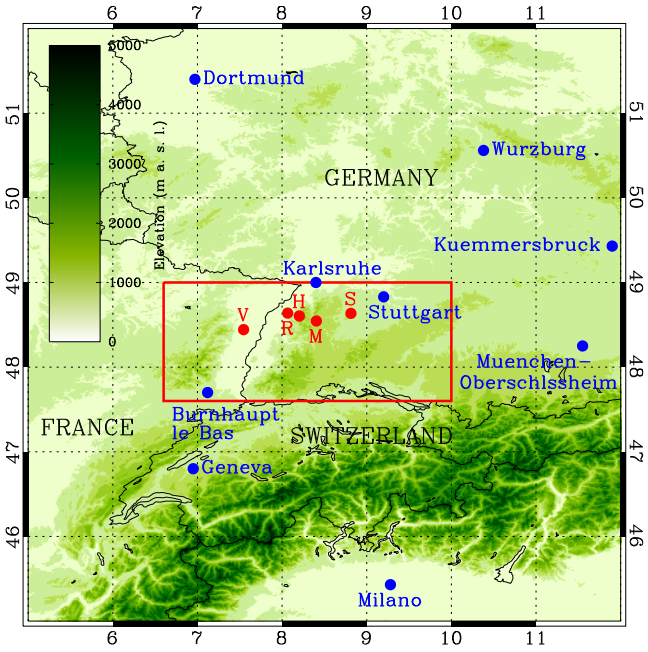

Figure 1. Map showing the "COPS area", which is indicated by the red rectangle. The supersites within the COPS region are labelled with red dots and are named after the areas that they represent: V - Vosges mountains; R - Rhine Valley (Achern); H - Hornisgrinde mountain; M - Murg Valley and; S - Stuttgart airport. The blue dots show the location of other radiosonde stations in the area.

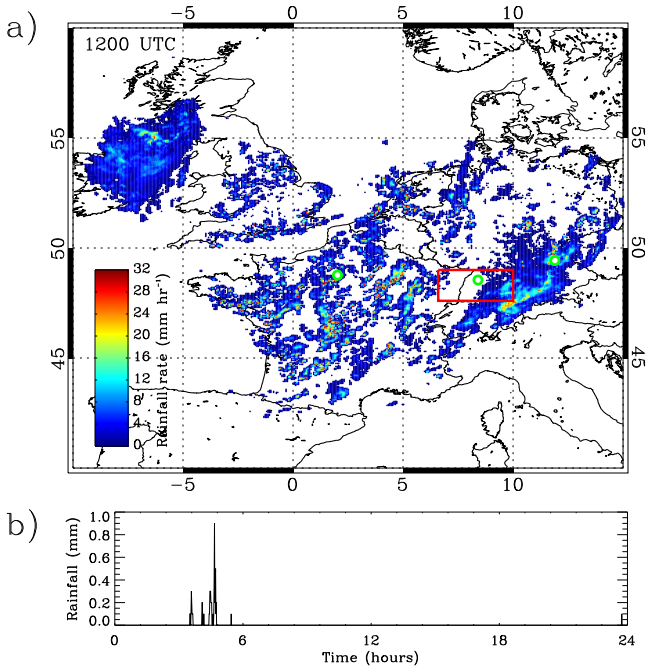

Figure 2. Precipitation during COPS IOP7b: a) Met Office NIMROD C-band radar showing rainfall rate at 1200 UTC indicating the intense but relatively small storms mainly over France, the large storms mainly over south-eastern Germany and the gap in precipitation over the COPS region, the green dots show the locations of Trappes, Achern and Kuemmersbruck respectively from west to east (soundings from these locations are shown in Fig. 6); and b) rain gauge data from Achern.

Prepared using qjrms3.cls
DOI: 10.1002/qj

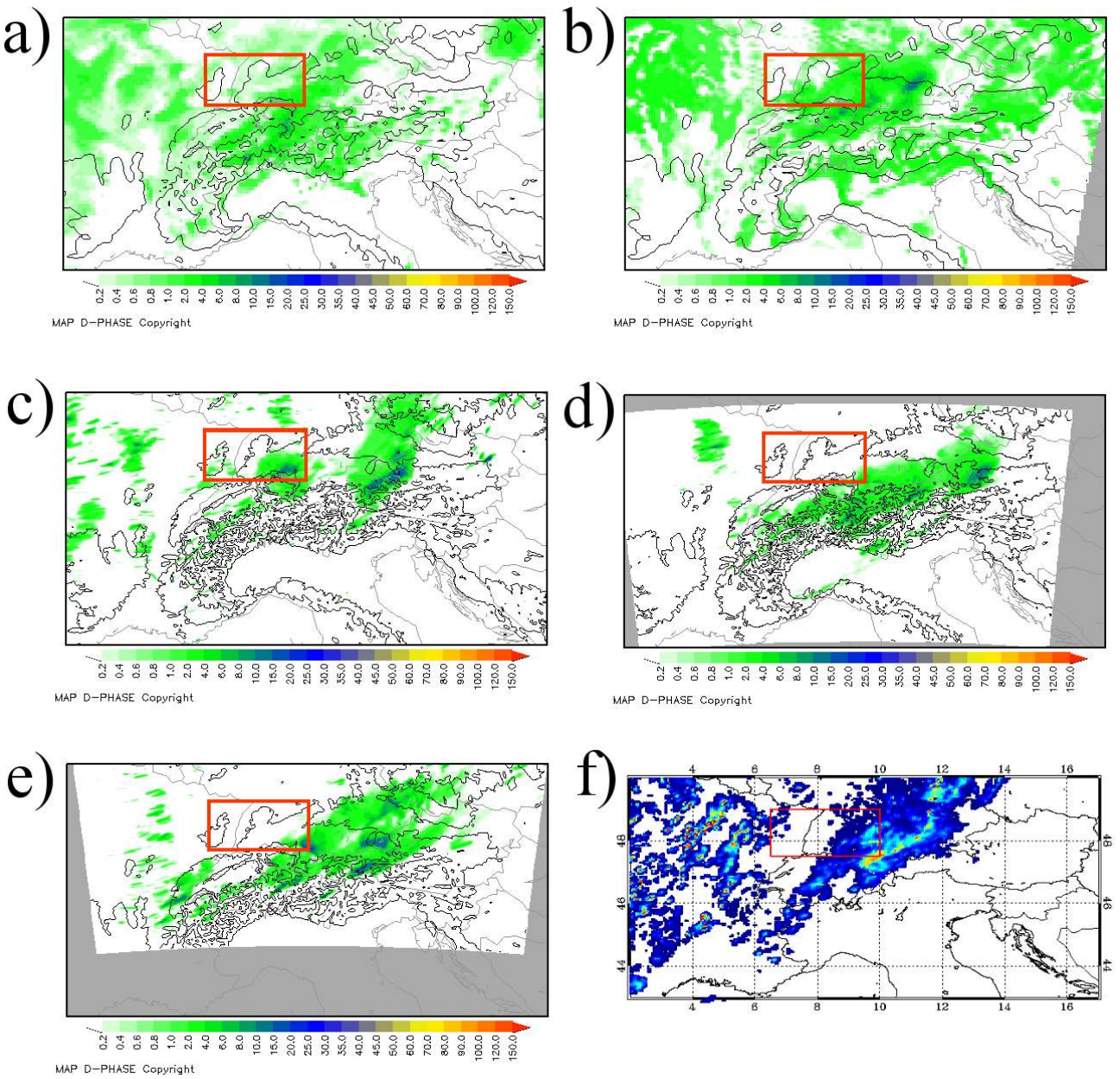

Figure 3. Modelled 1 hr accumulated precipitation (kg m^{-2}) from 1200 to 1300 UTC on 9 July 2007 from the following D-PHASE models (see Table I for details): a) ALADIN; b) MESO-NH; c) GEM-LAM; d) COSMO-CH and; e) COSMO-DE. f) shows the relevant area from the NIMROD rainfall radar (Fig. 2). The red rectangle indicates the COPS area.

Prepared using qjrms3.cls
DOI: 10.1002/qj

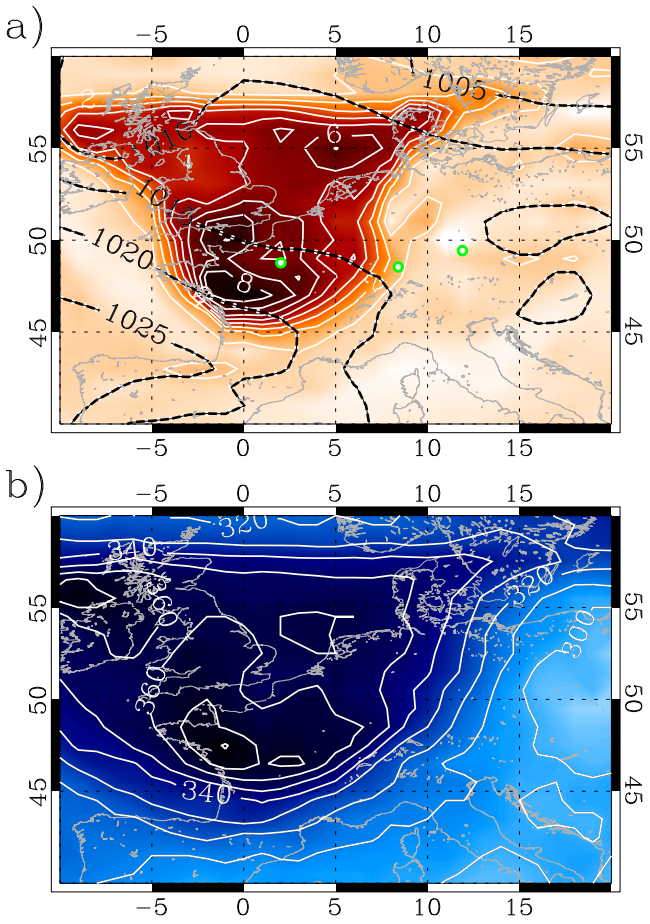

Figure 4. The upper-level PV anomaly shown by: a) ECMWF operational analysis of PV on the 315 K isentropic surface for 1200 UTC in PV units (PVU) i.e. 1.0×10^{-6} m^2 s^{-1} K kg^{-1} with mean sea level pressure (MSLP; dashed contours); and b) total ozone (in Dobson Units; DU) for ∼1130 UTC from TOMS, contours are plotted every 10 DU. Darker shading indicates higher levels of PV and O_3, respectively. a) also includes the location of the three soundings shown in Fig. 6.

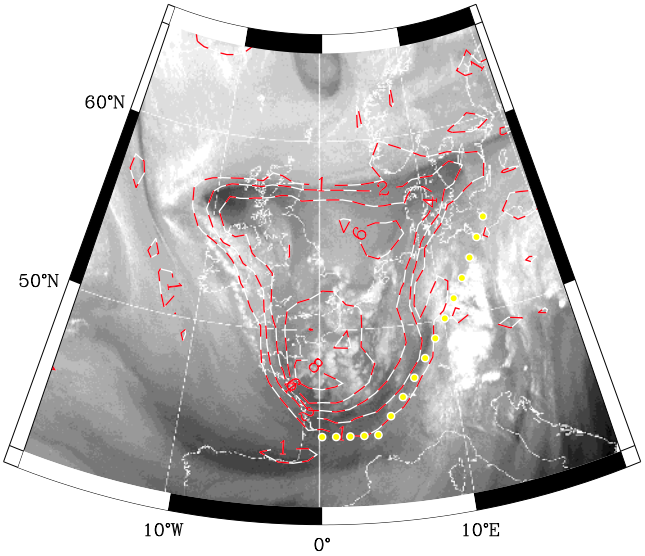

Figure 5. PV on the 315 K isentropic surface (red dashed contours; contour interval of 2 PVU from 2 to 8 PVU) at 1200 UTC plotted over the MSG water vapour image (©EUMETSAT 2007) for the same time. The yellow points show the path of the RH vertical cross section plotted in Fig. 12.

Prepared using qjrms3.cls
DOI: 10.1002/qj

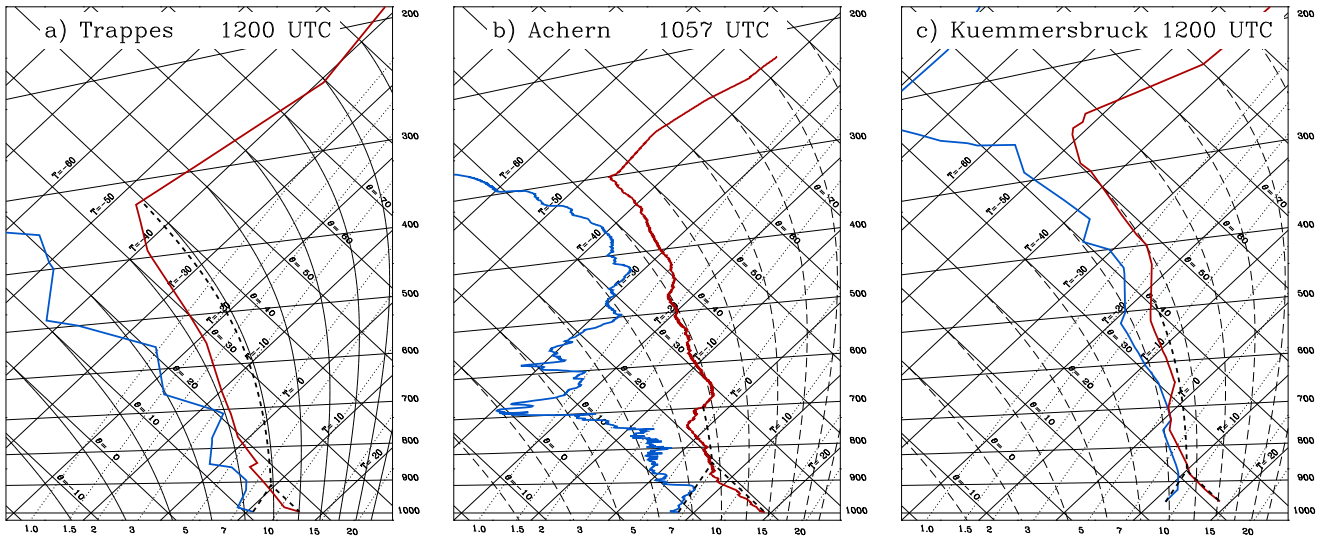

Figure 6. Tephigrams showing the three regimes: a) deep convection over Trappes (2.02°E, 48.77°N) at 1200 UTC; b) capping over Achern (8.07°E, 48.63°N) in the COPS region at 1057 UTC; and c) the widespread precipitation to the east of the COPS region over Kuemmersbruck (11.90°E, 49.43°N) at 1200 UTC. The tephigrams show dry bulb temperature (T; red line) and dew-point temperature (T_d; blue line). The lifted parcel trajectory has also been plotted (dashed line). The Trappes and Kuemmersbruck soundings are from the GTS network so are lower resolution.

DOI: 10.1002/qj

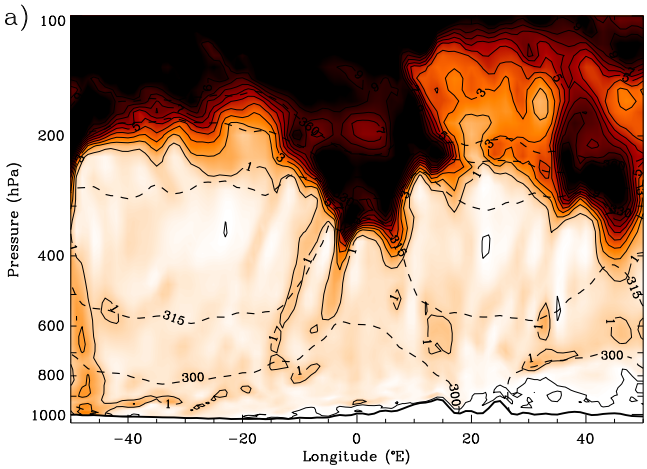

Figure 7. Vertical cross section of PV at 1200 UTC from the ECMWF operational analysis along 48°N i.e. approximately through the COPS supersites. Solid contours show PV in PV units (contour interval: 1 PVU). Darker shading represents higher PV. Dashed contours show potential temperature, also from the ECMWF operational analyses (contour interval: 15 K). The thick line towards the bottom of the plot shows the orography.

Prepared using qjrms3.cls
DOI: 10.1002/qj

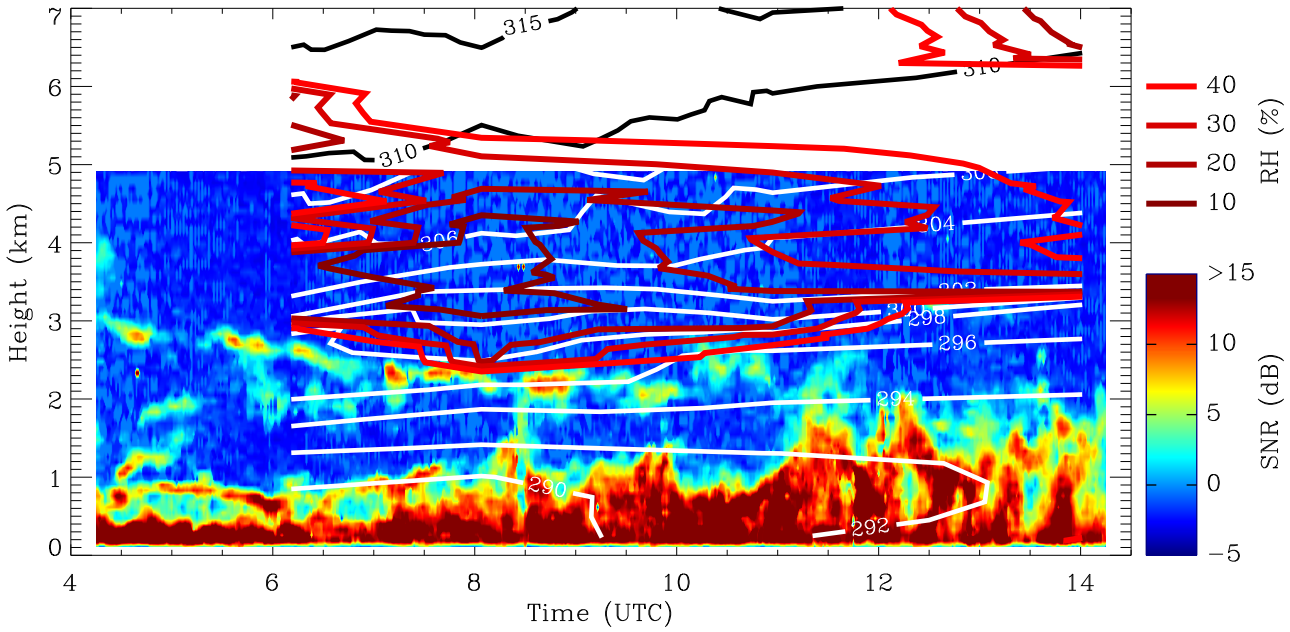

Figure 8. Signal to noise ratio (SNR) in dB from the UFAM UHF wind profiling radar located at Achern. The layer descending from 3.1 to 2.2 km between 0400 and 1200 UTC is the air mass gradient associated with the base of the main lid; and the growth of high echo power from lower levels during the day denotes the growth of the convective boundary layer. Potential temperature (black or white contours) and relative humidity (RH) below 40% (thick red contours) from four radiosondes (launched at 0611, 0804, 1057 and 1401 UTC from Achern, tephigrams available as Supplementary Material) have been overplotted.

Prepared using qjrms3.cls
DOI: 10.1002/qj

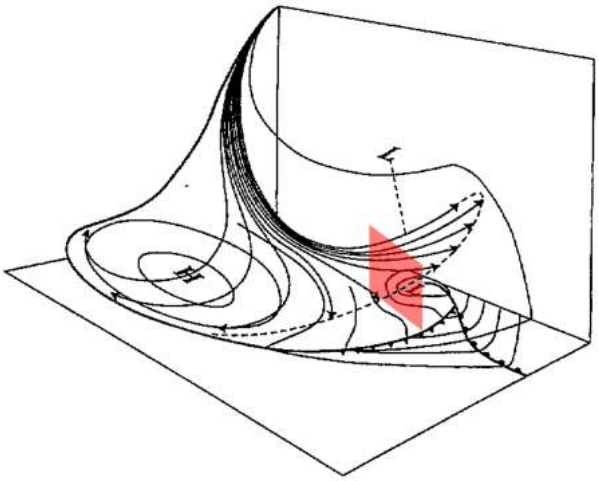

Figure 9. 3-D view of the dry intrusion from Danielsen (1964). The arrows show the path of air descending from the upper-troposphere and then partially re-ascending behind the cold front. The red shaded area represents an approximation of how the case examined in this paper aligns with the general flow described by the Danielsen model, in particular, Fig. 8 can be viewed as showing part of the shaded red cross section.

Prepared using qjrms3.cls
DOI: 10.1002/qj

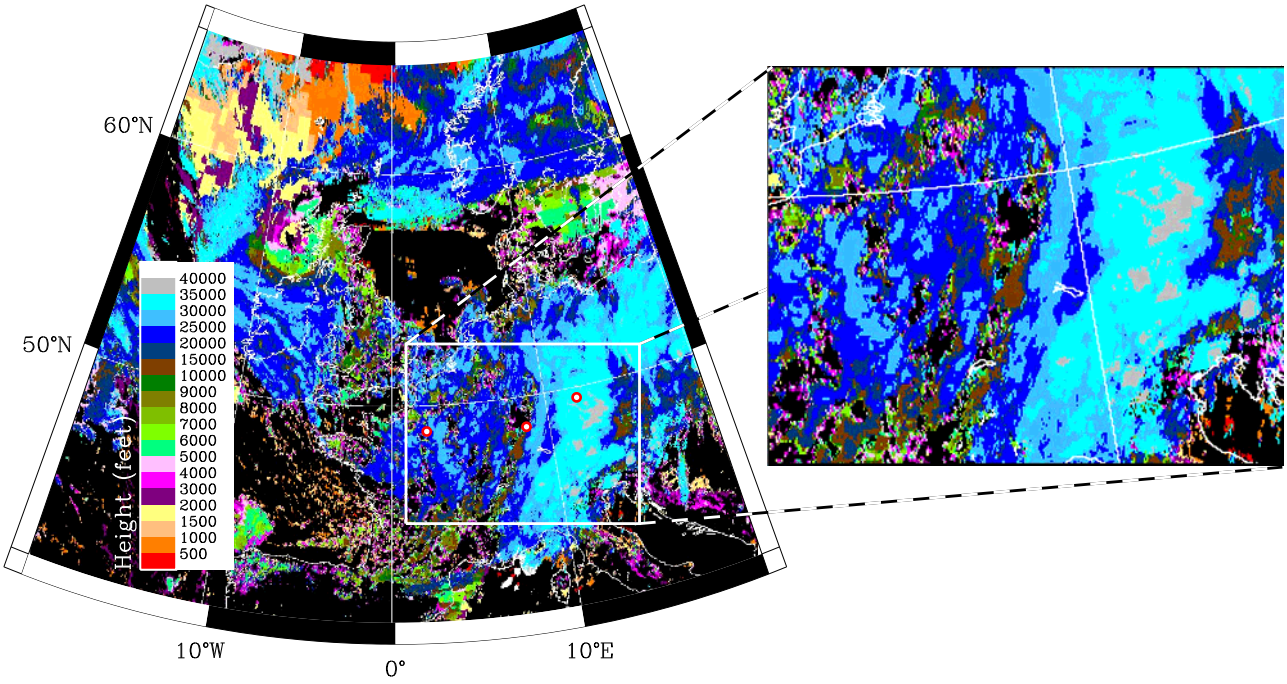

Figure 10. Cloud top height as calculated from the MSG satellite for 1400 UTC (©EUMETSAT 2007). The red dots show the locations of Trappes, Achern and Kuemmersbruck respectively from west to east. The area of interest has been magnified.

DOI: 10.1002/qj

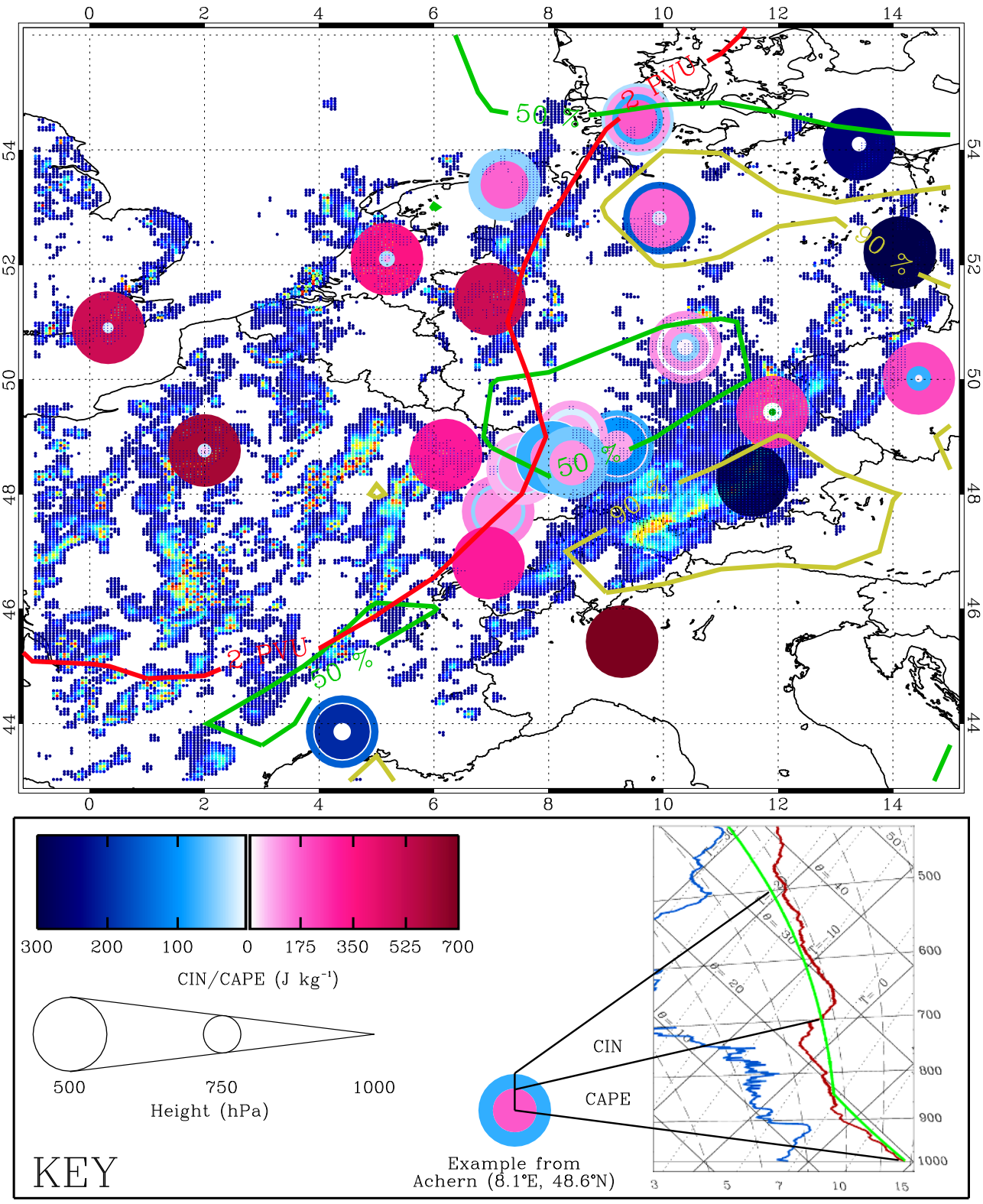

Figure 11. Map of CAPE and CIN indicated by circles/rings of different colour (see key) below 500 hPa. Height is indicated by circle/ring diameter (see scale). Values calculated from radiosondes launched at approximately 1200 UTC on 9 July 2007. An example of how the circle/rings have been constructed can be found in the key. They are plotted over Met Office NIMROD rainfall rate data (see Fig. 2 for scale) so that the regimes can be identified. ECMWF operational analyses of PV (2 PVU contour — red) and RH (50% RH (700 hPa) contour — green; 90% RH (900 hPa) contour — yellow) have also been used here to place the results into further context.

Prepared using qjrms3.cls
DOI: 10.1002/qj

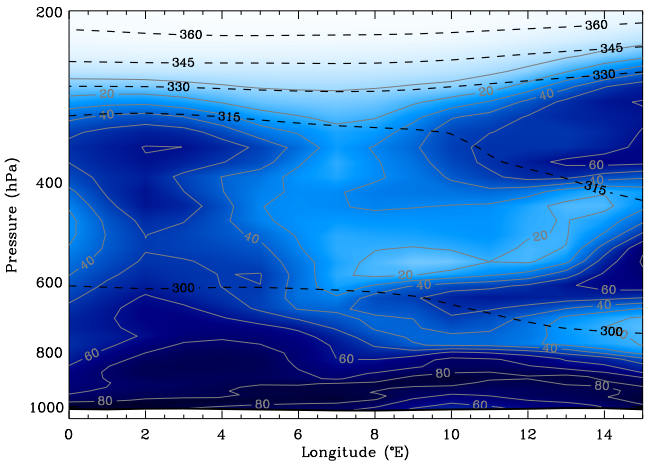

Figure 12. Vertical cross section of RH (%; contour interval is 10%) from the ECMWF operational analyses for 1200 UTC on 9 July 2007. The data is plotted along the line of yellow dots found on Fig. 5 i.e. from 0° to 4°E along the 44°N parallel and then northeastwards from 4°E, 44°N to 15°E, 55°N. This path was chosen as it skirts around the PV anomaly, which is the region most affected by the lid. The shading also represents RH where white is 0% and dark blue is 100% RH.

Prepared using qjrms3.cls
DOI: 10.1002/qj

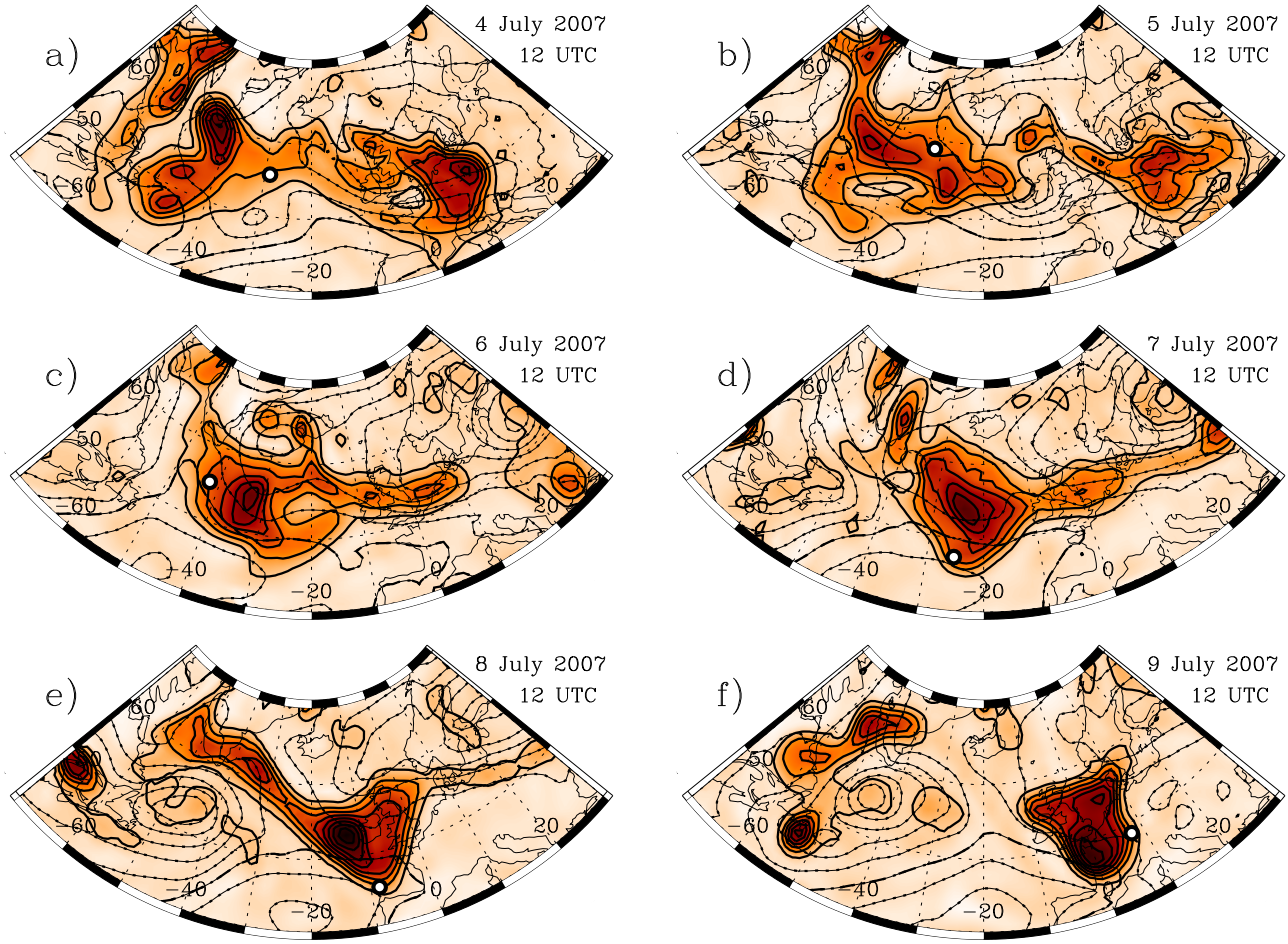

Figure 13. PV on the 315 K isentropic surface (solid contours and orange shading; contour interval of 1 PVU from 1 to 10 PVU) at 1200 UTC for the five days leading up to the IOP on 9 July 2007. MSLP is also plotted (dotted contours; contour interval of 5 hPa; the 1020 hPa contour is dot-dashed for reference). The white circle with a black outline plotted on each image identifies the location of the back trajectory associated with the main lid discussed in this paper (see Fig. 14).

Prepared using qjrms3.cls
DOI: 10.1002/qj

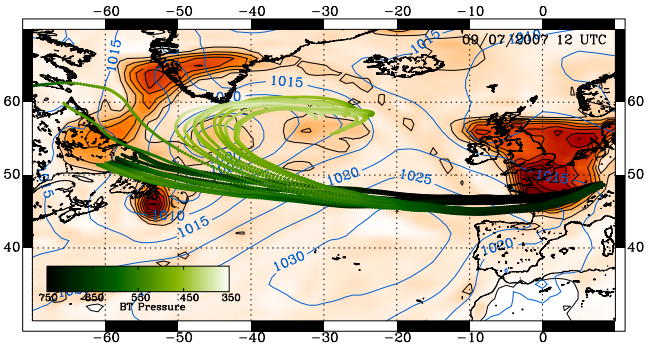

Figure 14. PV and MSLP plotted as in Fig. 13(f) with back trajectories relating to the main lid and base layer overplotted. The back trajectories were initiated as a cluster ($\pm$10 hPa, $\pm$0.33°N and $\pm$0.33°E) above Achern (8.07°E, 48.63°N) at the height of the warmest part of the main lid (660 hPa) and the base layer (725 hPa). This plot has also been provided as an animation available in the supplementary material.

Prepared using qjrms3.cls
DOI: 10.1002/qj

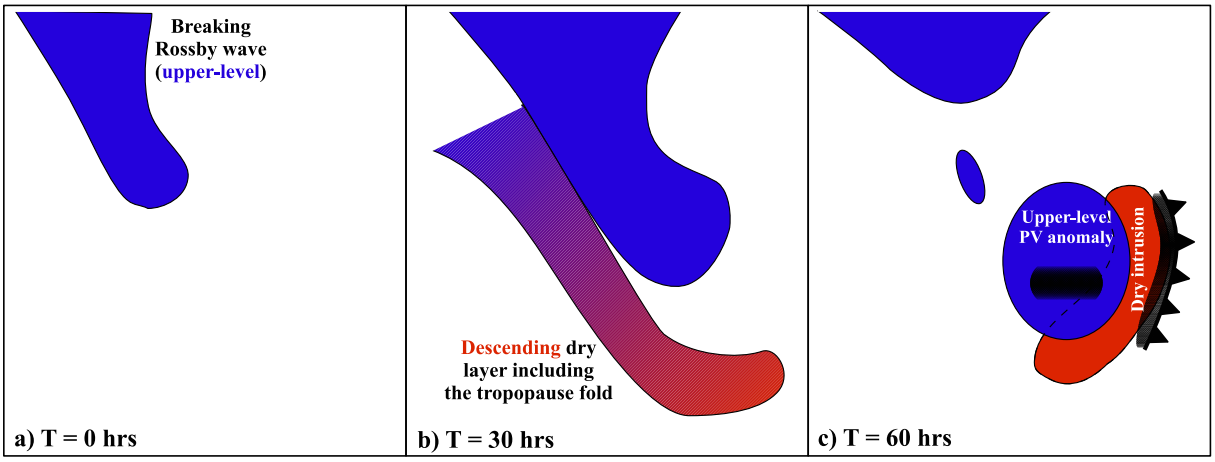

Figure 15. Conceptual model of the role and origin of the upper-level PV anomaly and the associated lid in the initiation of convection over western Europe — this has been developed from findings in this paper and Russell *et al.* (2008 and 2009). Upper-level features are shaded blue; lower-level features are shaded red. Hatched areas behind the front and beneath the PV anomaly indicate where precipitation is most likely but precipitation potential is not limited to those areas. In particular, the role of the dry layer in either inhibiting or promoting convection requires further investigation. The dry layer in panel c) is found in the mid- to low-troposphere so it is depicted as being partially beneath the PV anomaly. The scale of the PV anomaly in panel c) could be anything from 500 km (e.g. Russell *et al.*, 2008) to 1500 km (e.g. COPS IOP 7b — the case investigated here).

Prepared using qjrms3.cls
DOI: 10.1002/qj